Technology Research Center) support program (IITP-2015-H8501-15-1006) supervised by the IITP (Institute for Information & communications Technology Promotion).

REFERENCES

1. G.E. Ponchak and E. Tentzeris, Development of finite ground coplanar (FGC) waveguide 90 degree crossover junctions with low coupling, In: IEEE MTT-S International Microwave Symposium Digest, Boston, MA, 2000, pp. 1891–1894.
2. T.S. Hong, A rigorous study of microstrip crossovers and their possible improvements, IEEE Trans Microwave Theory Tech 42 (1994), 1802–1806.
3. J. Reed and G.J. Wheeler, A method of analysis of symmetrical four-port networks, IEEE Trans Microwave Theory Tech 4 (1956), 246–252.
4. D. Kholodniak, G. Kalinin, E. Vernoslova, and I. Vendik, Wideband 0-dB branch-line directional couplers, In: IEEE MTT-S International Microwave Symposium Digest, Boston, MA, 2000, pp. 1307–1310.
5. J.J. Yao, C. Lee, and S. Yeo, Microstrip branch-line couplers for crossover application, IEEE Trans Microwave Theory Tech 59 (2011), 87–92.
6. N.S.A. Arshad, et al., 0 dB coupler employing slot technique on planar microstrip.
7. Y. Chiou, J. Kuo, and H. Lee, Design of compact symmetric four-port crossover junction, IEEE Microwave Wireless Compon Lett 19 (2009), 545–447.
8. B. Henin and A. Abbosh, Design of compact planar crossover using sierpinski carpet microstrip patch, IET Microwave Antennas Propag 7 (2013), 54–60.
9. A. Abbosh, Planar wideband crossover with distortionless response using dual-mode microstrip patch, Microwave Opt Technol Lett 54 (2012), 2077–2079.
10. F.C. de Ronde, Octave-wide matched symmetrical reciprocal 4-and 5 ports, In: Proceedings of the IEEE MTT-S International Microwave Symposium Digest, Dallas, TX, 1982, pp. 521–523.
11. Y. Wang, A.M. Abbosh, and B. Henin, Broadband microwave crossover using combination of ring resonator and circular microstrip patch, IEEE Trans Compon Packaging Manuf Technol 3 (2013), 1771–1777.
12. J. Robinson and Y. Rahmat-Samii, Particle swam optimization in electromagnetics, IEEE Trans Antennas Propag, 59 (2002).
13. R.E. Collin, Foundations for microwave engineering, ch. 8, McGraw-Hill, New York, 1992.
14. K.W. Eccleston and S.H.M. Ong, Compact planar microstripline branch-line and rat-race couplers, IEEE Trans Microwave Theory Tech 51 (2003), 2119–2125.
15. HFSS: High frequency structure simulator based on finite element method, v. 15.0 ANSYS Corp., Pittsburgh, PA, 2013.

DUAL-WIDEBAND U-SHAPE OPEN-SLOT ANTENNA FOR THE LTE METAL-FRAMED TABLET COMPUTER

Kin-Lu Wong and Chih-Yu Tsai
Department of Electrical Engineering, National Sun Yat-Sen University, Kaohsiung 80424, Taiwan; Corresponding author: wongkl@ema.ee.nsysu.edu.tw

Received 6 April 2015

ABSTRACT: *The open-slot antenna is very suitable for applications in the metal-framed tablet device, such as the tablet computer, to achieve a low profile with wideband or multiband operation. This article presents a U-shape open-slot (U-slot) antenna with a low profile of 7 mm to the top edge of the metal-framed tablet computer for the LTE operation. The U-slot has a simple structure of length 70 mm and the two slot openings thereof are disposed at the metal frame. The U-slot antenna is fed using an end-shorted 50-Ω microstrip feedline, with a wideband matching network embedded therein. The antenna can support a 0.5-wavelength slot resonant mode supported by the U-slot itself and a 0.25-wavelength slot resonant mode created by the open-slot radiator (denoted as Slot 1 in this study) formed between one slot opening and the microstrip feedline as a virtual shorting. By further using an inverted-U strip connecting across the U-slot, the antenna can create an additional open-slot radiator (denoted as Slot 2 in this study) to generate a 0.25-wavelength slot resonant mode at lower frequencies. The resonant modes supported by the U-slot, Slot 1, and Slot 2 can form two wideband operating bands to cover the LTE operation in the 698–960 and 1710–2690 MHz bands. Details of the proposed U-slot antenna and the effects of the inverted-U strip connecting across the U-slot and the matching network are addressed. Experimental results of the fabricated U-slot antenna are also presented.* © 2015 Wiley Periodicals, Inc. Microwave Opt Technol Lett 55:2677–2683, 2015; View this article online at wileyonlinelibrary.com. DOI 10.1002/mop.29421

Key words: *mobile antennas; open-slot antennas; slot antennas; tablet computer antennas; LTE antennas; dual-wideband antennas*

1. INTRODUCTION

The tablet communication device such as the tablet computer is becoming very slim in its appearance to meet the demands of the mobile users. For such slim tablet computers, a metal frame is usually added around the edges thereof to increase the robustness of the device. The metal frame, however, will cause significant effects on the conventional antennas such as the inverted-F antennas or monopole antennas embedded near the edges of the device so as to fit in the narrow spacing between the display panel and edges thereof [1]. Conversely, for such metal-framed communication devices, the slot antenna can take advantages of the metal frame as part of the antenna, thereby making it promising to have a low antenna profile yet capable of wideband or multiband operation for the mobile communications [2].

In the recent study in [2], a linear open-slot antenna with two slot openings can have a low profile of 10 mm to the top edge of the metal-framed mobile handset and generate two wide operating bands to cover the LTE (long term evolution) operation in the 698–960 and 1710–2690 MHz bands [3]. In this article, we present a U-shape open-slot (U-slot) antenna with a low profile of 7 mm to the top edge of the metal-framed tablet computer for the LTE operation. The low profile makes it easy for the antenna to fit in the narrow spacing between the display panel and the top edge of the metal-framed tablet computer.

In addition, different from the linear open-slot antenna studied in [2] in which two open-slot radiators are created, the proposed U-slot antenna can support three open-slot radiators for the LTE operation. The three open-slot radiators include the U-slot itself, a short open slot (Slot 1) between a first slot opening and the microstrip feedline as a virtual shorting, and a long open slot (Slot 2) between a second slot opening and an inverted-U strip added to connect across the U-slot. With the aid of a wideband matching circuit, the three open-slot radiators (U-slot, Slot 1, and Slot 2) generate their fundamental slot resonant modes to form two wide operating bands to cover the desired 698–960 and 1710–2690 MHz bands for the LTE operation [2–9].

In this study, the antenna structure and operating principle of the proposed U-slot antenna are addressed. Effects of the inverted-U strip added in the U-slot to create an additional open-slot radiator (Slot 2) and the wideband matching circuit

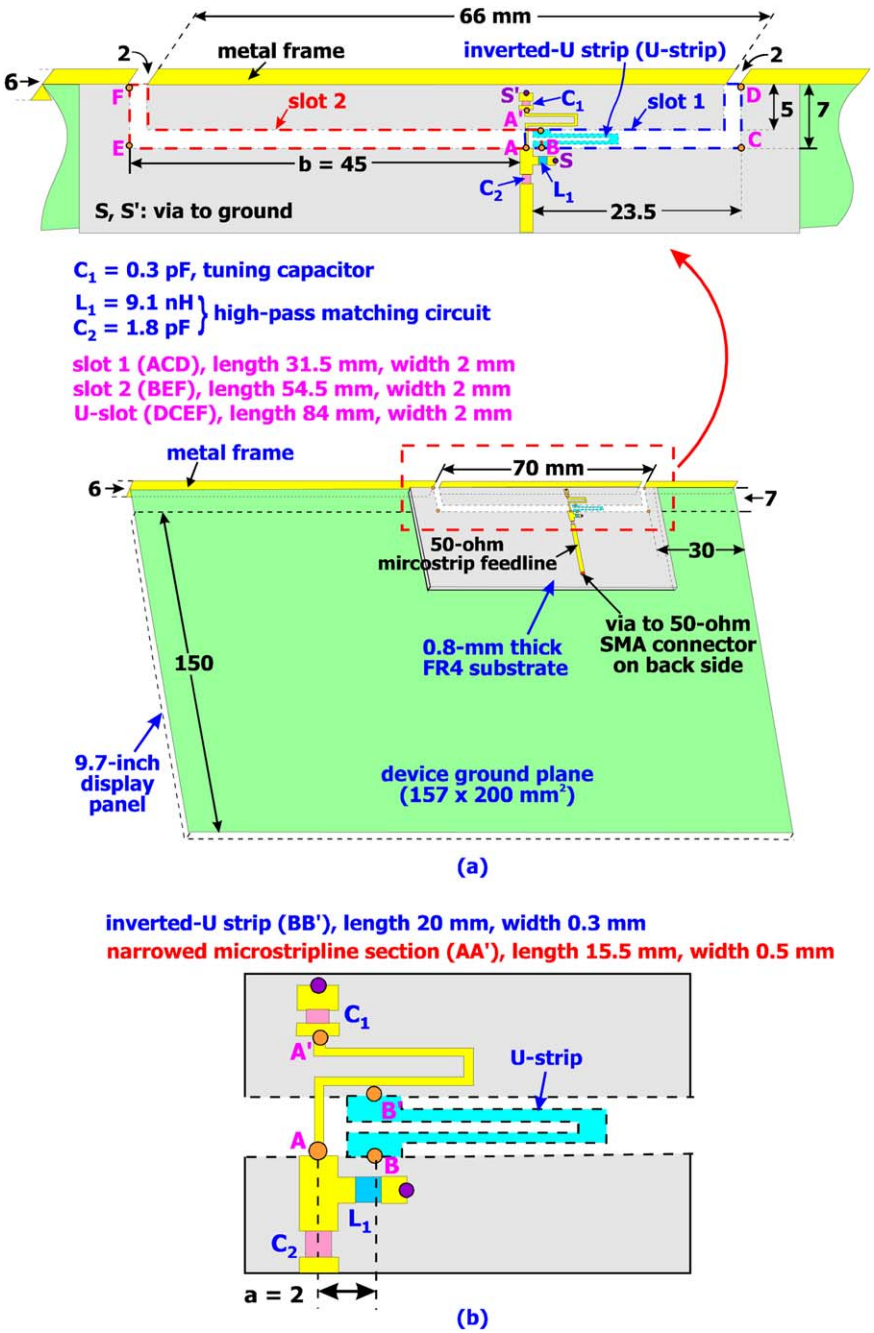

Figure 1 (a) Geometry of the dual-wideband U-shape open-slot (U-slot) antenna for the LTE tablet computer. (b) Enlarged view of the feeding network (C_1, C_2, L_1) and the inverted-U strip (U-strip) connecting across the U-slot. [Color figure can be viewed in the online issue, which is available at wileyonlinelibrary.com]

embedded in the microstrip feedline are discussed. A parametric study is also conducted to analyze the effects of the position variations of the microstrip feedline and the inverted-U strip on the antenna performance. The U-slot antenna is also fabricated, and the experimental results are presented and discussed.

2. PROPOSED U-SLOT ANTENNA

2.1. Antenna Structure

Figure 1(a) shows the geometry of the dual-wideband U-shape open-slot (U-slot) antenna for the LTE tablet computer. An enlarged view of the feeding network and the inverted-U strip (denoted as U-strip in the study) connecting across the U-slot are shown in Figure 1(b). The U-slot antenna is disposed in the narrow spacing of 7 mm between the display panel and top edge of the metal-framed tablet computer. Note that in the study, the device ground plane is selected to have a size of 157 × 200 mm^2, which is a typical size for the popular tablet computer with a 9.7-inch display panel. In the experiment, the device ground plane is cut from a 0.2-mm thick copper plate. The display panel is not included in the simulation and experimental studies.

The U-slot antenna has two slot openings of width 2 mm in the metal frame at the top edge of the device ground plane. The U-slot antenna is fabricated on a 0.8-mm thick FR4 substrate of relative permittivity 4.4 and loss tangent 0.02. The ground plane of the U-slot antenna is connected to the device ground plane, which is

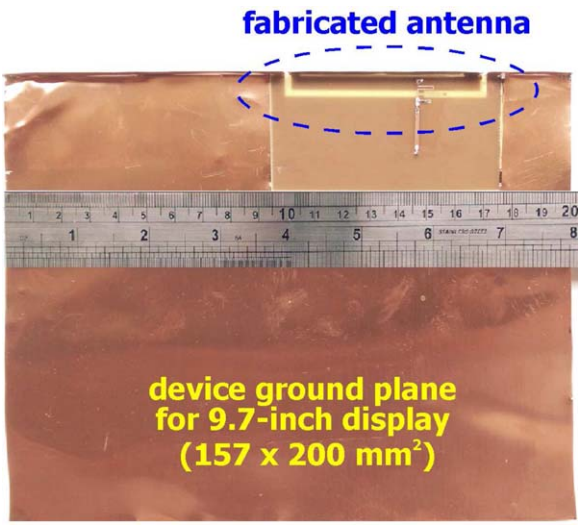

Figure 2 Photos of the fabricated antenna. [Color figure can be viewed in the online issue, which is available at wileyonlinelibrary.com]

also connected to the 6-mm wide metal frame as shown in the figure. To show the antenna structure more clearly, the photos of the fabricated antenna are presented in Figure 2. Note that for practical cases, the metal frame is usually disposed at all the four edges of the metal-framed tablet computer. In the antenna structure shown in Figure 1(a), only the metal frame at the top edge is added so as to simplify the study. The obtained results, however, are expected to be in general the same as the case with the metal frame added at all the four edges. Also note that one slot opening of the U-slot is disposed at about the center of the top edge, where the magnetic field distribution is generally maximum for the dipole-like chassis (device ground plane) mode, which can lead to good excitation of the desired slot resonant modes [10,11].

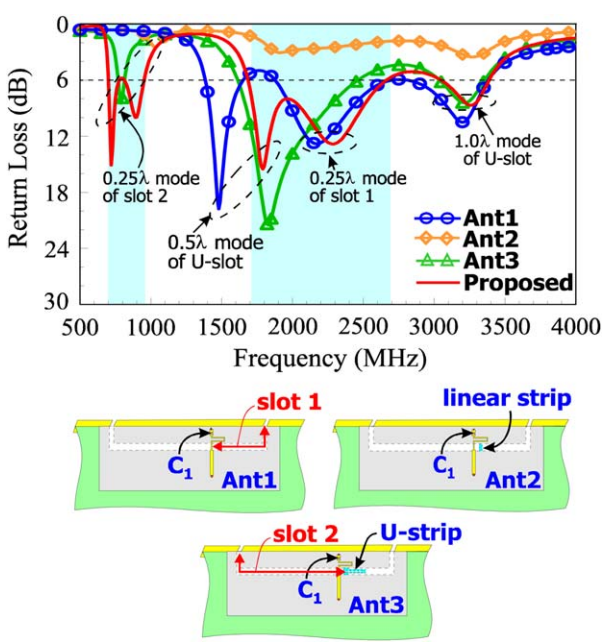

Figure 3 Simulated return loss for the proposed U-slot antenna, the case without the U-strip across the U-slot and the high-pass matching circuit of L_1 and C_2 (denoted as Ant1), Ant1 with a simple linear strip connecting across the U-slot (Ant2), and Ant2 with the U-strip connecting across the U-slot (Ant3). [Color figure can be viewed in the online issue, which is available at wileyonlinelibrary.com]

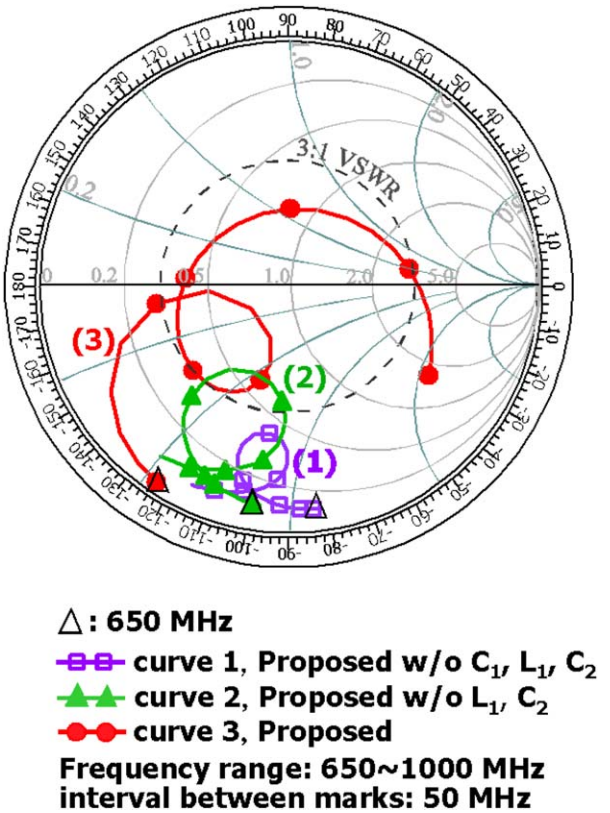

Figure 4 Simulated input impedance on the Smith chart for the proposed antenna without C_1, L_1, and C_2 (Curve 1), the proposed antenna without L_1 and C_2 (Curve 2), and the proposed antenna (Curve 3) in the frequency range of 650–1000 MHz. [Color figure can be viewed in the online issue, which is available at wileyonlinelibrary.com]

The U-slot has a slot width of 2 mm and a slot length of 84 mm (section DCEF), while the length of the U-slot along the top edge is 70 mm. Through the excitation of the end-shorted 50-Ω microstrip feedline [2,12], the U-slot itself can generate a 0.5-wavelength slot resonant mode in the antenna's desired

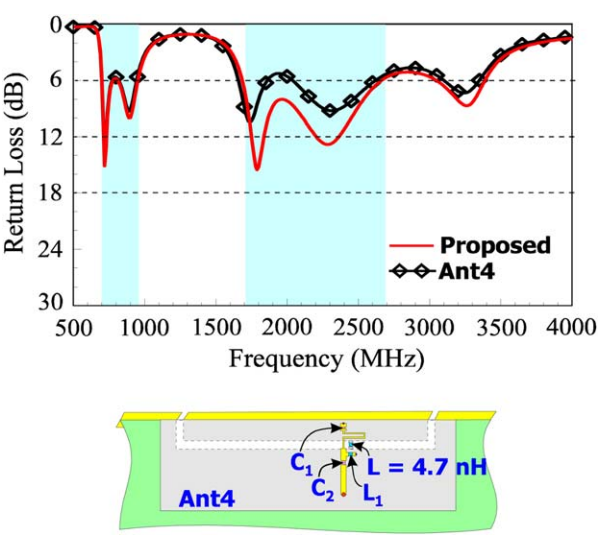

Figure 5 Simulated return loss for the proposed antenna and the case with a 4.7-nH chip inductor replacing the U-strip connecting across the slot (Ant4). [Color figure can be viewed in the online issue, which is available at wileyonlinelibrary.com]

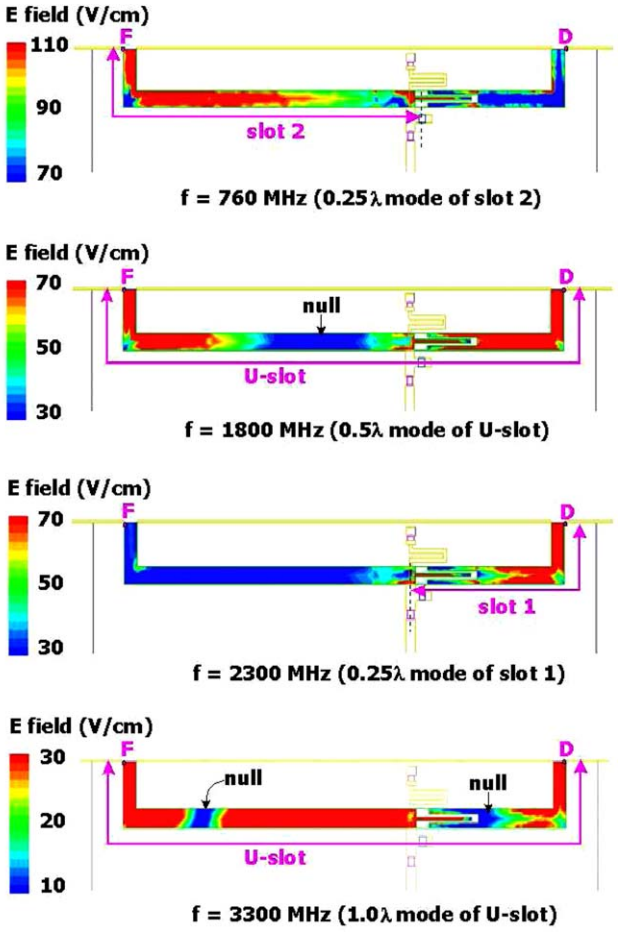

Figure 6 Simulated electric-field distributions in the U-slot. [Color figure can be viewed in the online issue, which is available at wileyonlinelibrary.com]

higher band. This excited 0.5-wavelength slot resonant mode in this study has strong electric fields at the two slot openings and a null electric field at about the slot center, which is different from the traditional 0.5-wavelength closed-slot resonant mode [13] and will be discussed with the aid of Figure 6 later.

A 0.25-wavelength slot resonant mode [2,14–17] can also be generated by Slot 1 of length 31.5 mm (section ACD), which is the slot region between the slot opening at point D and the microstrip feedline as a virtual shorting [18]. The 0.5-wavelength U-slot mode and the 0.25-wavelength Slot-1 mode are formed into a very wide higher band for the antenna to cover the desired 1710–2690 MHz band.

By adding an inverted-U strip (denoted as U-strip here) across the U-slot, an additional open-slot radiator (Slot 2) of length 54.5 mm (section BEF) is formed. The U-strip (section BB′) has a length of 20 mm and a width of 0.3 mm. This U-strip functions like a distributed inductor, which leads to a lengthened resonant length of Slot 2. A similar result can be obtained by replacing the U-strip using a chip inductor of 4.7 nH, which will be discussed with the aid of Figure 5 later. With the present of the U-strip, a 0.25-wavelength slot resonant mode contributed by Slot 2 can be generated at about 800 MHz, with small effects on the generation of the slot modes contributed by the U-slot and Slot 1. By further aided with the high-pass matching circuit of L_1 (9.1 nH) and C_2 (1.8 pF) in the microstrip feedline, the antenna's lower band can be widened to cover the desired 698–960 MHz band. Also note that the capacitor C_1 (0.3

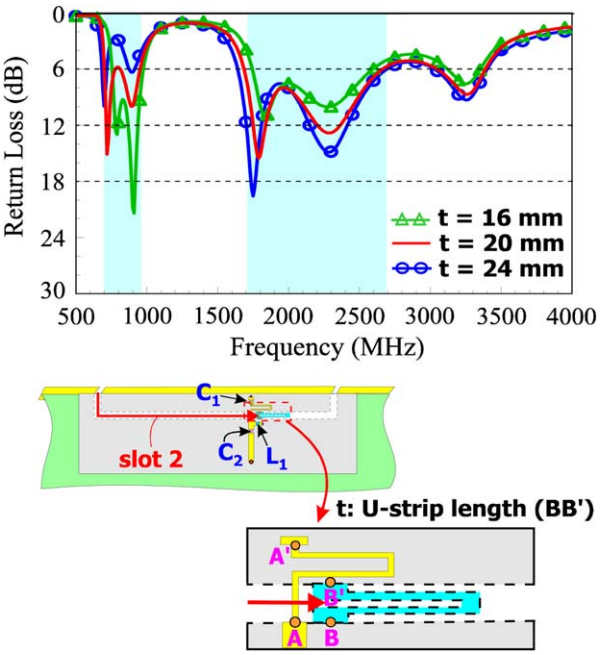

Figure 7 Simulated return loss for the proposed antenna with different lengths of the U-strip connecting across the U-slot. [Color figure can be viewed in the online issue, which is available at wileyonlinelibrary.com]

pF) added near point S′ is used to compensate for the equivalent inductance owing to the end-shorting of the microstrip feedline. The narrowed strip section AA′ following the capacitor C_1 and passing across the U-slot has a length of 20 mm and a width of 0.5 mm, which can effectively fine-tune the impedance matching of the antenna [2].

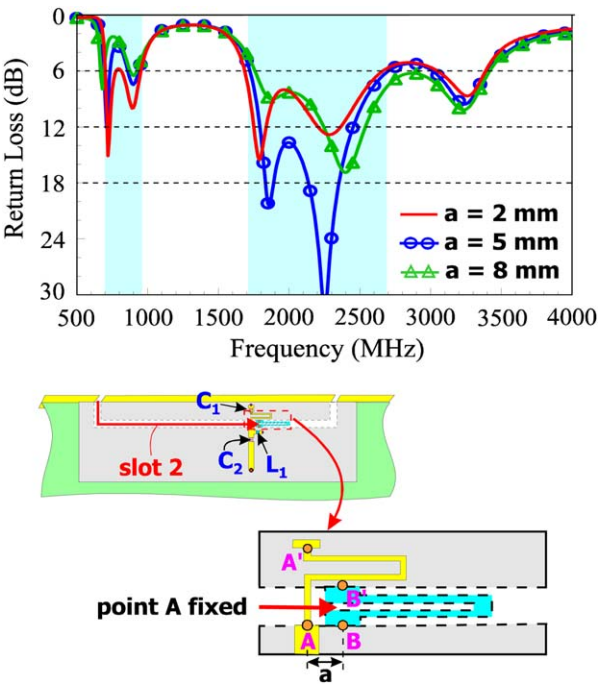

Figure 8 Simulated return loss for the proposed antenna with different positions of the U-strip connecting across the U-slot, with the position of the microstrip feedline fixed (point A fixed). [Color figure can be viewed in the online issue, which is available at wileyonlinelibrary.com]

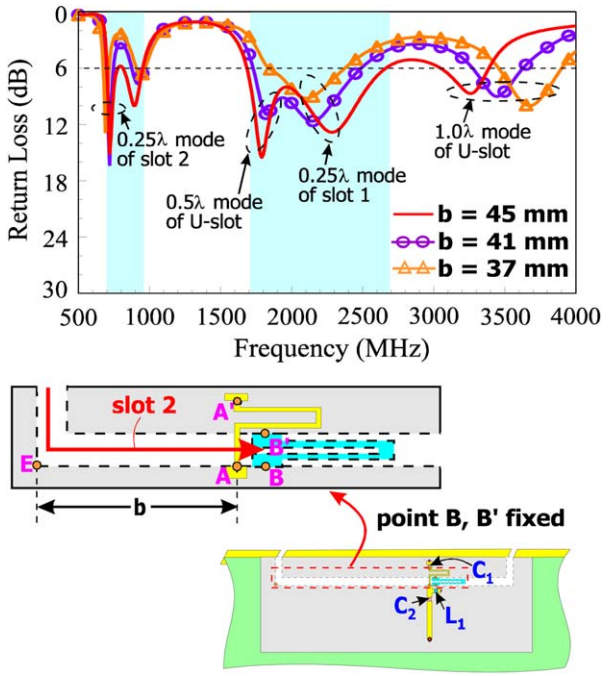

Figure 9 Simulated return loss for different positions of the microstrip feedline passing across the U-slot, with the position of the U-strip fixed (point B, B′ fixed). [Color figure can be viewed in the online issue, which is available at wileyonlinelibrary.com]

2.2. Operating Principle

Figure 3 shows the simulated return loss for the U-slot antenna, the case without the U-strip across the U-slot and the high-pass matching circuit of L_1 and C_2 (denoted as Ant1), Ant1 with a simple linear strip connecting across the U-slot (Ant2), and Ant2 with the U-strip connecting across the U-slot (Ant3). The simulated results are obtained using the full-wave electromagnetic field simulator HFSS version 15 [19]. For Ant1, it is seen that the U-slot and Slot 1 contribute their slot resonant modes at about 1.5 GHz (0.5-wavelength U-slot mode), 2.2 GHz (0.25-wavelength Slot-1 mode), and 3.2 GHz (1.0-wavelength U-slot mode). No resonant modes are excited in the desired lower band. The desired lower and higher bands are marked in color in the figure. For Ant2, the presence of a simple linear strip significantly degrades the impedance matching of the resonant modes contributed by the U-slot and Slot 1. Using the U-strip connecting across the U-strip (that is, Ant3), it is seen that a

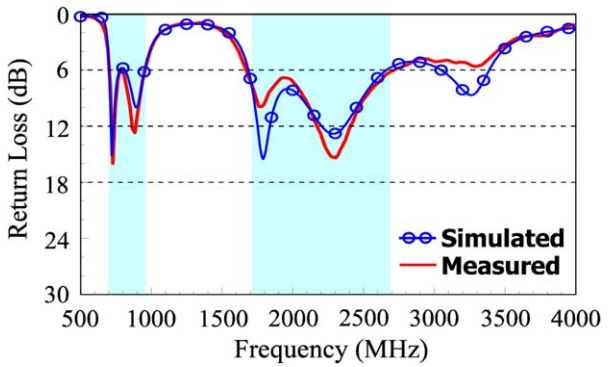

Figure 10 Measured and simulated return losses for the fabricated antenna. [Color figure can be viewed in the online issue, which is available at wileyonlinelibrary.com]

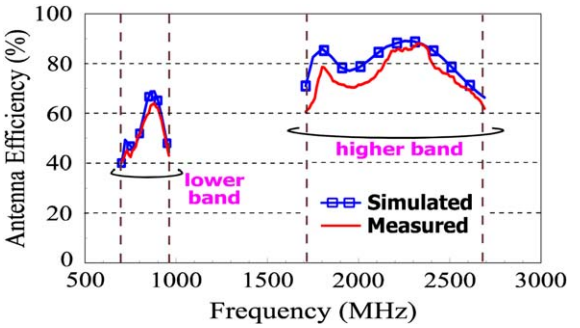

Figure 11 Measured and simulated antenna efficiencies for the fabricated antenna. [Color figure can be viewed in the online issue, which is available at wileyonlinelibrary.com]

new resonant mode occurs at about 800 MHz in the desired lower band and the resonant modes contributed by the U-slot and Slot 1 remain excited with good impedance matching. By adding the high-pass matching circuit to Ant3 (that is, the proposed antenna), widened bandwidth in the antenna's lower band is obtained to cover the 698–960 MHz, and the resonant modes contributed by the U-slot and Slot 1 can also be formed into the desired higher band of 1710–2690 MHz.

Effects of the matching network embedded in the microstrip feedline for the bandwidth enhancement in the antenna's lower band are studied with the aid of Figure 4. The simulated input impedance on the Smith chart for the proposed antenna without C_1, L_1, and C_2 (Curve 1), the proposed antenna without L_1 and C_2 (Curve 2), and the proposed antenna (Curve 3) in the frequency range of 650–1000 MHz are shown. For Curve 1, the impedance matching is poor in the desired lower band. By adding the capacitor C_1, which compensates for the end-shorting effects of the microstrip feedline, much improved impedance matching is seen (see Curve 2 vs. Curve 1). When the high-pass matching circuit is added, a looped impedance curve within the 3:1 VSWR circle is seen (see Curve 3), which indicates that a dual-resonance excitation for the widened bandwidth in the desired lower band is obtained.

Figure 5 shows the simulated return loss for the proposed antenna and the case with a chip inductor replacing the U-strip connecting across the slot (Ant4). It is seen that Ant4 has a similar return loss as that of the proposed antenna. This behavior suggests that the U-strip mainly functions like a distributed inductor, which creates a new open-slot radiator (Slot 2) and also causes small effects on the existing slot radiators of the U-slot and Slot 1. Hence, additional resonant modes can be obtained to achieve widened bandwidth for the antenna to cover the LTE operation in both the 698–960 and 1710–2690 MHz bands.

Figure 6 shows the simulated electric-field distributions in the U-slot of the proposed antenna. At 760 MHz, the excited electric-field distribution is strong at the slot opening of point F and decreases gradually to the position of the U-strip. The result indicates that resonant mode at 760 MHz is a 0.25-wavelength slot mode [2] contributed by Slot 2. At 1800 and 3300 MHz, the excited electric-field distributions suggest that the corresponding resonant modes are 0.5-wavelenth and 1.0-wavelength slot modes contributed by the U-slot. At 2300 MHz, strong electric field is excited at the slot opening of point D and is mainly contributed by Slot 1. In the proposed antenna, three open-slot radiators of the U-slot, Slot 1, and Slot 2 contribute their fundamental resonant modes to form two wide operating bands for the desired LTE operation in the 698–960 and 1710–2690 MHz bands.

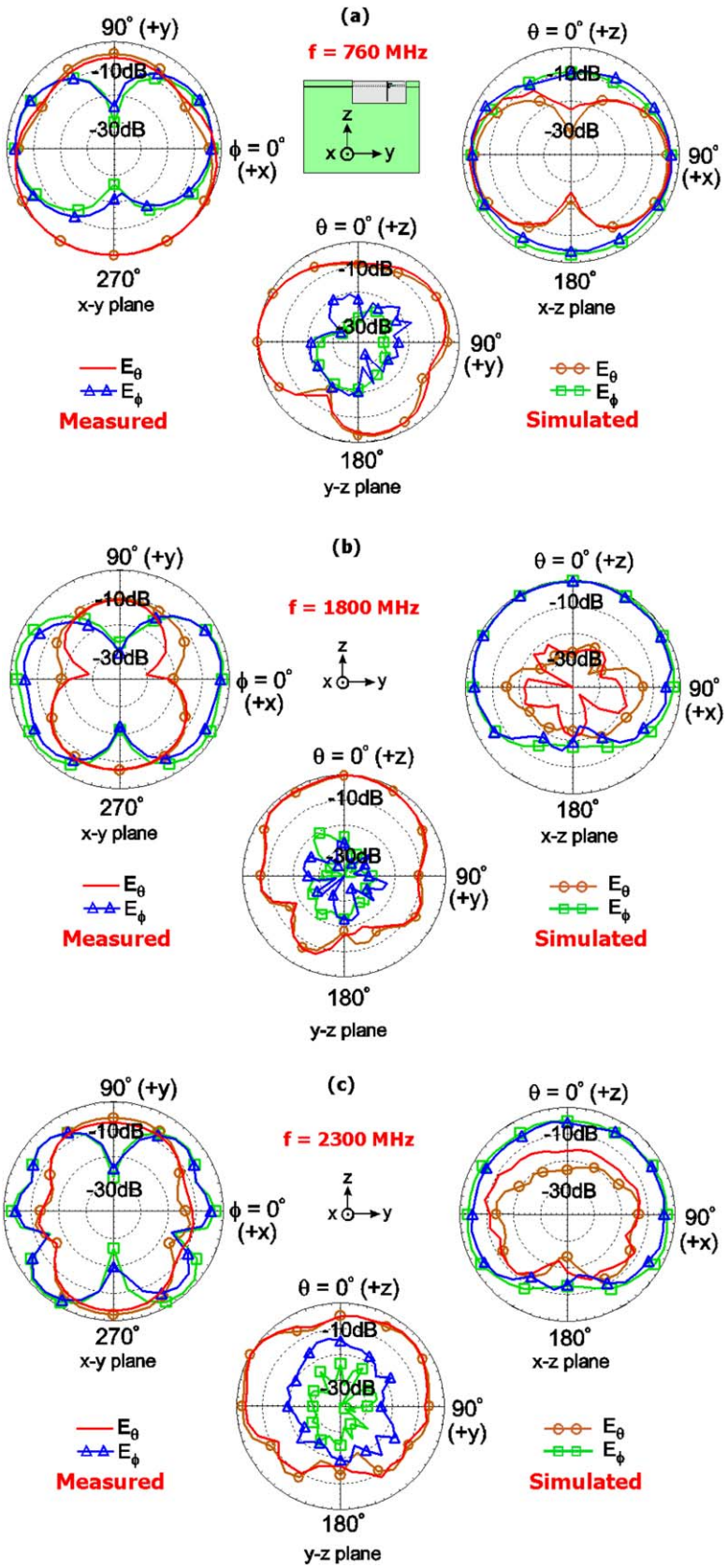

Figure 12 Measured and simulated radiation patterns for the fabricated antenna. (a) 760 MHz (b) 1800 MHz and (c) 2300 MHz. [Color figure can be viewed in the online issue, which is available at wileyonlinelibrary.com]

2.3. Parametric Study

The simulated return-loss results for the length t of the U-strip varied from 16 to 24 mm are shown in Figure 7. Other parameters are the same as given in Figure 1. Large effects on the excited resonant mode in the antenna's lower band are seen. The first resonant mode in the lower band, which is contributed

by Slot 2, is also seen to be shifted to lower frequencies with an increase in the length t. This suggests that the resonant mode contributed by Slot 2 can be adjusted by tuning the length of the U-strip, which is selected to be 20 mm in this study.

Figure 8 shows the simulated return loss for the position of the U-strip varied from 2 to 5 mm away from the microstrip feedline at point A. Similar as observed in Figure 7, large effects on the first resonant mode in the antenna's lower band are seen. When the distance a increases, the first resonant mode is shifted to lower frequencies. This is reasonable, as the first resonant mode is contributed by Slot 2, a larger distance of a causes a longer resonant length of Slot 2, thereby shifting the excited mode to lower frequencies.

Figure 9 shows the simulated return loss for different positions of the microstrip feedline across the U-slot, with the position of the U-strip fixed (point B, B′ fixed). Results for the distance b varied from 37 to 45 mm are shown. It is seen that all the resonant modes contributed by the U-slot, Slot 1, and Slot 2 are greatly affected. This is largely because all the three slot radiators are excited by the microstrip feedline. Hence, the position variations of the microstrip feedline will cause effects on all their contributed resonant modes.

3. EXPERIMENTAL RESULTS

The proposed U-slot antenna was fabricated (see the photos shown in Fig. 2) and tested. Figure 10 shows the measured and simulated return losses for the fabricated antenna. The measured data agree well with the simulated results. The impedance matching of the frequencies in the desired LTE bands is seen to be better than 6 dB (3:1 VSWR). The measured and simulated antenna efficiencies for the fabricated antenna are presented in Figure 11. The radiation characteristics of the antenna were measured in a far-field anechoic chamber. The antenna efficiencies include the mismatching loss. Agreement between the measurement and simulation is also generally seen. The measured antenna efficiencies are about 40–63% and 60–86% for the desired lower and higher bands, respectively. The obtained antenna efficiencies are generally acceptable for practical mobile communication applications [20,21].

Figure 12 shows the measured and simulated radiation patterns at representative frequencies of 760, 1800, and 2300 MHz. The radiation patterns in the x-y plane (the azimuthal plane), the x-z plane (the elevation plane orthogonal to the device ground plane), and the y-z plane (the elevation plane parallel to the device ground plane) are plotted. The measured radiation patterns are also seen to be similar to the corresponding simulated results. At 760 MHz, stronger radiation in the $-y$ direction in the x-y plane and in the $-z$ direction in the x-z plane is seen, which suggests that the device ground plane also contributes to the radiation. That is, the dipole-like chassis (device ground plane) mode is also excited at lower frequencies. At 1800 and 2300 MHz, stronger radiation in the upper half-plane in the elevation planes (x-z and y-z planes) is seen, which suggests that the device ground plane mainly functions as a reflector more than a radiator at higher frequencies.

4. CONCLUSION

A dual-wideband U-shape open-slot antenna for the LTE operation in the metal-framed tablet computer has been proposed, fabricated, and studied. The antenna has a simple structure with a low profile of 7 mm yet exhibits a dual-wideband operation to cover the 698–960 and 1710–2690 MHz for the LTE operation. It has been demonstrated that by embedding a U-strip connecting across the U-slot, three open-slot radiators (the U-slot, Slot 1, and Slot 2) can contribute their fundamental resonant modes to form the dual-wideband operation. Acceptable radiation characteristics for the antenna have also been obtained. The proposed U-slot antenna is promising for applications in modern slim metal-framed tablet computers, especially for those having a narrow spacing between the metal frame and the display panel thereof.

REFERENCES

1. B. Yuan, Y. Cao, G. Wang, and B. Cui, Slot antenna for metal-rimmed mobile handsets, IEEE Antennas Wireless Propag Lett 11 (2012), 1334–1337.
2. K.L. Wong and P.R. Wu, Dual-wideband linear open slot antenna with two open ends for the LTE/WWAN smartphone, Microwave Opt Technol Lett 57 (2015), 1269–1274.
3. LTE frequency bands and spectrum allocations, Available at: http://www.radio-electronics.com/.
4. K.L. Wong and Z.G. Liao, Passive reconfigurable triple-wideband antenna for LTE tablet computer, IEEE Trans Antennas Propag 63 (2015), 901–908.
5. Y.L. Ban, S.C. Sun, P.P. Li, J.L.W. Li, and K. Kang, Compact eight-band frequency reconfigurable antenna for LTE/WWAN tablet computer applications, IEEE Trans Antennas Propag 62 (2014), 471–474.
6. K.L. Wong and L.Y. Chen, Small-size LTE/WWAN tablet device antenna with two hybrid feeds, IEEE Trans Antennas Propag 62 (2014), 2926–2934.
7. K.L. Wong and C.Y. Tsai, Small-size stacked inverted-F antenna with two hybrid shorting strips for the LTE/WWAN tablet device, IEEE Trans Antennas Propag 62 (2014), 3962–3969.
8. J.H. Lu and Y.S. Wang, Planar small-size eight-band LTE/WWAN monopole antenna for tablet computers, IEEE Trans Antennas Propag 62 (2014), 4372–4377.
9. K.L. Wong and C.Y. Tsai, Combined-type triple-wideband LTE tablet computer antenna, Microwave Opt Technol Lett 57 (2015), 1262–1267.
10. H. Wang, M. Zheng, and S.Q. Zhang, Monopole slot antenna, US Patent No. 6618020 B2, September 9, 2003.
11. P. Linberg, E. Ojefors, and A. Rydberg, Wideband slot antenna for low-profile handheld terminal applications, In: Proceedings of 36th European Microwave Conference, Manchester, UK, 2006, pp. 1698–1701.
12. Z. Liu and K. Boyle, Bandwidth enhancement of a quarter-wavelength slot antenna by capacitive loading, Microwave Opt Technol Lett 51 (2009), 2114–2115.
13. R. Bancroft, Dual slot radiating single feedpoint printed circuit board antenna, US Patent No. 7129902 B2, October 31, 2006.
14. C.I. Lin and K.L. Wong, Printed monopole slot antenna for internal multiband mobile phone antenna, IEEE Trans Antennas Propag 55 (2007), 3690–3697.
15. K.L. Wong and L.C. Lee, Multiband printed monopole slot antenna for WWAN operation in the laptop computer, IEEE Trans Antennas Propag 57 (2009), 324–330.
16. K.L. Wong, P.W. Lin, and C.H. Chang, Simple printed monopole slot antenna for penta-band WWAN operation in the mobile handset, Microwave Opt Technol Lett 53 (2011), 1399–1404.
17. K.L. Wong and W.J. Lin, WWAN/LTE printed slot antenna for tablet computer application, Microwave Opt Technol Lett 54 (2012), 44–49.
18. N. Behdad and K. Sarabandi, A multiresonant single-element wideband slot antenna, IEEE Antennas Wireless Propag Lett 3 (2004), 5–8.
19. Available at: http://www.ansys.com/products/hf/hfss/, ANSYS HFSS.
20. K.L. Wong and M.T. Chen, Very-low-profile dual-wideband loop antenna for LTE tablet computer, Microwave Opt Technol Lett 57 (2015), 141–146.
21. K.L. Wong and Z.G. Liao, Small-size dual-wideband monopole antenna with inductive and capacitive feeding branches for long term evolution tablet computer application, Microwave Opt Technol Lett 57 (2015), 853–860.